

[Al₄(OH)₂(OCH₃)₄(H₂N-bdc)₃]_xH₂O: A 12-Connected Porous Metal–Organic Framework with an Unprecedented Aluminum-Containing Brick**

Tim Ahnfeldt, Nathalie Guillou, Daniel Gunzelmann, Irene Margiolaki, Thierry Loiseau, Gérard Férey, Jürgen Senker, and Norbert Stock*

The search for new, highly porous, and thermally and chemically stable compounds has been one of the main objectives of many investigations in recent years.^[1–3] Metal–organic frameworks (MOFs) present the ideal class of compounds to achieve this target, as they are built up from inorganic bricks and organic complexing molecules. Their modular assembly provides the possibility to adjust pore sizes and to fine-tune the shape and functionality of the pores.^[4] One important requirement is the reproducible formation of the inorganic bricks.^[1] Once the reaction conditions for the inorganic unit have been established, the variation of the organic linker should in principle allow the synthesis of isorecticular compounds using larger or functionalized organic molecules. Thus, many MOF structures depend on the presence of defined inorganic building units. Often paddle-wheel units (e.g. {Cu₂(O₂CR)₄}), for example in HKUST-1,^[5] or tetranuclear {Zn₄O} tetrahedra (as in the IRMOF series or MOF-177)^[6,7] are observed. Trimeric building units {M₃(μ₃-O)(O₂CR)₆} are found in a series of MOFs, for instance those based on the MIL-88 topology as well as MIL-100 and MIL-101.^[8,9] Recently, rigid carboxylate linkers were used to connect substituted polyoxotungstates under hydrothermal conditions to form inorganic–organic frameworks.^[10] We were able to synthesize iron-containing MIL-53, MIL-88, and MIL-

101 based on Fe^{III} and aminoterephthalate^[11] as well as the large-pore analogue of MIL-101, which contains naphthylidicarboxylic acid instead of terephthalic acid as the organic unit.^[12] In this context, the use of high-throughput methods has been shown to be a valuable tool for the systematic and efficient investigation of hydrothermal reaction systems. Such systematic investigations in the field of inorganic–organic hybrid compounds are still rare,^[13–17] although different reagents, reaction stoichiometries, and process parameters have a strong influence on the product formation.

Aluminum-based MOFs are known to show good thermal stabilities (up to 450–500 °C for Al-MIL-53).^[18] From a structural point of view, different Al-based MOFs can be formed from distinct inorganic bricks (Figure 1). MIL-96 is

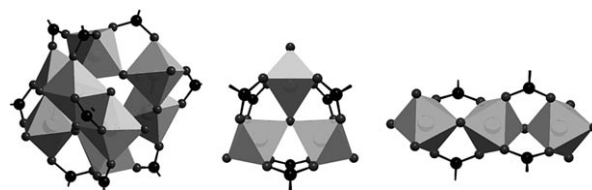


Figure 1. Inorganic Al-containing bricks in Al-containing MOFs. Left: octanuclear {Al₈(OH)₁₅(O₂CR)₉} cluster in MIL-110. Center: trinuclear {Al₃(μ₃-O)(O₂CR)₆} cluster in MIL-96. Right: corner-sharing {AlO₆} octahedra in MIL-96, MIL-69, and MIL-53.

built up from isolated trinuclear {Al₃(μ₃-O)(O₂CR)₆} clusters and corrugated chains of corner-sharing aluminum octahedra, which form a honeycomb lattice containing 18-membered rings.^[19] MIL-110 contains octanuclear {Al₈(OH)₁₅(O₂CR)₉} clusters arranged in a honeycomb lattice.^[20] A number of compounds, such as MIL-53^[18,21] and MIL-69,^[22,23] are based on chains of corner-sharing aluminum octahedra that are connected to form one-dimensional rhombic channels. We have been able to synthesize amine-functionalized Al-MIL-53 and to use it in a postsynthetic modification reaction.^[24] Recently, Al-MIL-53-NH₂ was shown to be a stable, highly active, basic catalyst in a Knoevenagel condensation, and to be well-suited for CO₂/CH₄ separation.^[25,26]

Herein we present the results of our systematic investigation of the system Al³⁺/aminoterephthalic acid (H₂N-H₂bdc)/solvent, which led to the new 12-connected, highly porous, and stable metal–organic framework [Al₄(OH)₂(OCH₃)₄(H₂N-bdc)₃]_xH₂O (named CAU-1; CAU = Chris-

[*] T. Ahnfeldt, Prof. Dr. N. Stock

Institut für Anorganische Chemie, Christian-Albrechts-Universität
 Max-Eyth-Strasse 2, 24118 Kiel (Germany)
 Fax: (+49) 431-880-1775
 E-mail: stock@ac.uni-kiel.de

Dr. N. Guillou, Dr. T. Loiseau, Prof. Dr. G. Férey
 Institute Lavoisier, UMR 8637 CNRS
 Université de Versailles-Saint Quentin
 45 Avenue des États-Unis, 78035 Versailles (France)

D. Gunzelmann, Prof. Dr. J. Senker
 Anorganische Chemie I, Universität Bayreuth
 Universitätsstrasse 30, 95447 Bayreuth (Germany)

Dr. I. Margiolaki
 European Synchrotron Radiation Facilities, ID31
 Materials Science Group, Inorganic Chemistry I
 6, rue Jules Horowitz, BP 220, 38043 Grenoble (France)

[**] The work has been supported by the State of Schleswig-Holstein and the Deutsche Forschungsgemeinschaft (DFG) through the priority program SPP 1362 “Porous Metal–Organic Frameworks” under grants STO 643/5-1 and SE 1417/4-1. bdc = benzene dicarboxylate.

Supporting information for this article is available on the WWW under <http://dx.doi.org/10.1002/ange.200901409>.

tian-Albrechts-University), containing the new Al-containing octameric brick $\{Al_8(OH)_4(OCH_3)_8\}^{12+}$.

In the course of the systematic investigation of the formation of new or functionalized isorecticular aluminum-containing MOFs, high-throughput experiments were performed with various chemical and process parameters.^[11,14,17] Thus, the influence of the molar ratios of starting compounds, the solvents, and the use of different aluminum salts on the product formation in the system $Al^{3+}/H_2N-H_2bdc/solvent$ was studied (Figure 2). Three Al^{3+}/H_2N-H_2bdc molar ratios (1:2, 1:1, and 2:1) were used in four different solvents. On the basis of the results of previous studies,^[24] a reaction temperature of 125 °C and reaction time of 5 h were chosen as starting parameters.

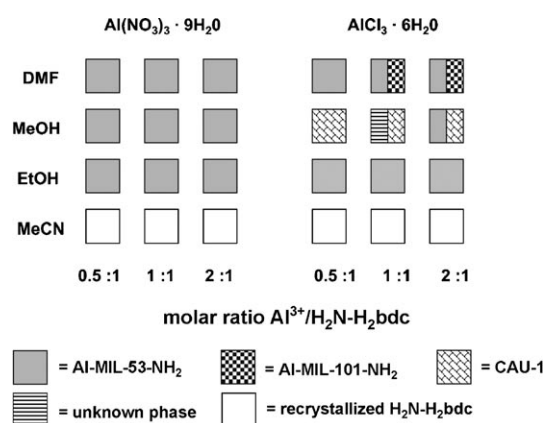


Figure 2. Results of the high-throughput investigation of the system $Al^{3+}/H_2N-H_2bdc/solvent$ at 125 °C.

The solvents have the most profound influence on product formation. In acetonitrile, only recrystallized aminoterephthalic acid is recovered, while in ethanol poorly crystalline Al-MIL-53-NH₂ is formed. The use of DMF or methanol as the reaction medium increases the complexity of the system. With $Al(NO_3)_3 \cdot 9H_2O$ as the starting material, the formation of Al-MIL-53-NH₂ is observed in both solvents. Reaction mixtures containing $AlCl_3 \cdot 6H_2O$ as the starting material result in the formation of new phases. In addition to the well-known phase Al-MIL-53-NH₂,^[24] for the first time Al-containing MIL-101 is observed. The latter is formed in DMF at molar ratios $Al^{3+}/H_2N-H_2bdc \geq 1$. The reactions in methanol yielded an unidentified phase and the title compound CAU-1, $[Al_4(OH)_2(OCH_3)_4(H_2N-bdc)_3] \cdot xH_2O$ (see Figure S1 in the Supporting Information for all XRD patterns). The synthesis procedure was optimized using high-throughput methods (see the Supporting Information), and a procedure for gram-scale reactions was established.

The crystal structure of CAU-1 was determined from powder X-ray diffraction data (Figure 3, Tables S1 and S2 in the Supporting Information).^[27] High-precision powder X-ray diffraction data were collected on ID31 of the European Synchrotron Radiation Facilities (ESRF). Extractions of the peak positions, pattern indexing, Fourier calculations, and Rietveld refinements were carried out with the TOPAS program.^[28] A tetragonal unit cell was found unambiguously

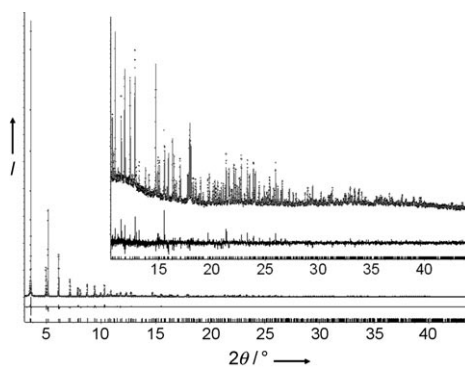


Figure 3. Final Rietveld plot of the structure refinement of $[Al_4(OH)_2(OCH_3)_4(H_2N-bdc)_3] \cdot xH_2O$ (CAU-1). The observed data are shown by dots and the calculated pattern by a solid line. The difference curve is represented below; vertical bars mark the Bragg reflection positions. The inset shows a plot enlargement for $2\theta > 12^\circ$.

with satisfactory figure of merit ($GoF = 110$) using the LSI indexing method. Systematic extinctions were consistent with the I Bravais lattice, and the $I4/mmm$ space group was chosen to solve the structure. Calculations were performed with the EXPO package,^[29] using EXTRA^[30] for extracting integrated intensities and SIR97^[31] for direct-methods structure solution.

The tetragonal structure of CAU-1 is built up from a pseudo-body-centered-cubic arrangement of the 8-ring building blocks $\{Al_8(OH)_4(OCH_3)_8\}^{12+}$ (Figure 4), which are linked by 12 aminoterephthalate ions.^[32] The wheel-shaped 8-rings are built from corner- and edge-sharing $\{AlO_6\}$ polyhedra

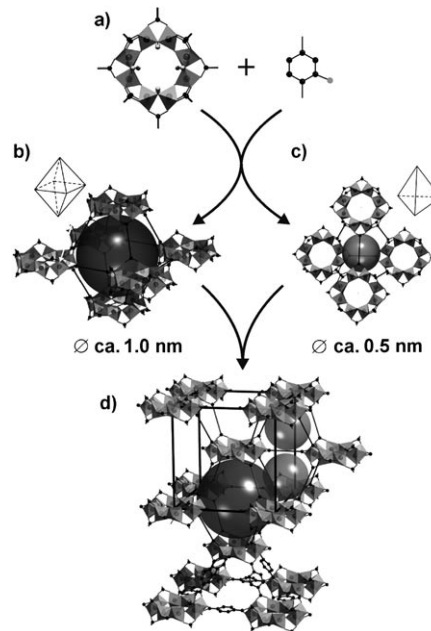


Figure 4. Structure of CAU-1. The brick $\{Al_8(OH)_4(OCH_3)_8\}^{12+}$ is formed by corner- and edge-sharing AlO_6 octahedra (a). These wheel-shaped bricks are connected to 12 other units through the aminoterephthalate linker. Thus, distorted octahedral (b) and tetrahedral (c) cages are formed. The structure (d) can be derived from a tetragonally distorted cubic centered cell. For clarity, some of the phenyl rings are replaced by straight lines, and the disordered NH_2 groups are omitted.

through the hydroxide and methoxide groups, respectively. The Al^{3+} ion resides on a unique crystallographic site and is coordinated to three carboxylate oxygen atoms, one hydroxide, and two methoxide ions. Each wheel is connected to 12 other units by aminoterephthalate linkers with four linkers in the plane of the 8-ring as well as four above and four below the ring. Thus, a three-dimensional microporous framework is formed with two types of cages, distorted octahedral and distorted tetrahedral, with effective accessible diameters of approximately 1 and 0.45 nm, respectively, taking into account the van der Waals radii of the carbon atoms. Access to the cages is only possible through small triangular windows with a free aperture of 0.3–0.4 nm. The disordered water molecules are located close to the middle of the 8-ring units and are involved in hydrogen bonds.

Both the occurrence of an 8-ring unit and the presence of a 12-connected net are notable. Very similar octameric rings with edge- and corner-sharing alternation have been observed for vanadium, chromium, and iron in vanadium hydroxide carboxylates $[\text{V}_8(\text{OH})_4(\text{OEt})_8(\text{O}_2\text{Ac})_{12}]^{[33]}$ and $[\text{V}_8(\text{OH})_4(\text{OEt})_8(\text{O}_2\text{CPh})_{12}]^{[34]}$ chromium hydroxide acetate $[\text{Cr}_8(\text{OH})_{12}(\text{O}_2\text{Ac})_{12}] \cdot 34 \text{H}_2\text{O}^{[35]}$ and iron hydroxide carboxylate $[\text{Fe}_8(\text{OH})_8(\text{OPh})_8(\text{O}_2\text{CR})_{12}]$ ($\text{R} = \text{Bu}$ or Ph),^[36] but it is novel in aluminum chemistry. Moreover, the wheel-type analogues involving transition metals are isolated as discrete molecular clusters, whereas the octanuclear Al-based unit in CAU-1 is fully connected to generate an infinite three-dimensional framework. Such 12-connected metal–organic frameworks are very rare,^[37–39] and recently such a net was observed in the zirconium-based MOF UiO-66, which contains $\{\text{Zr}_6\text{O}_4(\text{OH})_4(\text{CO}_2)_{12}\}$ units. This structure represents an expanded version of the cubic close-packed structure.^[40]

For a more detailed characterization, IR, Raman, and multinuclear solid-state NMR spectroscopic studies (Figures S2 and S3 in the Supporting Information) as well as thermogravimetric analysis (TGA) and elemental analysis were carried out. Especially the high-resolution ^{13}C and ^{15}N NMR spectra unequivocally demonstrate the incorporation of methoxide ions (^{13}C H_3CO^- $\delta = 48$ ppm) and aminoterephthalate (^{15}N NH_2 $\delta = -327$ ppm) into the structure of CAU-1. The methyl groups of the methoxide ions are also clearly detectable in the IR and Raman spectrum.

The TGA data of CAU-1 show a two-step weight loss. The first step, with a weight loss of 6.3% in the temperature range of 25–100°C, corresponds to the release of three water molecules per formula unit, whereas only one water molecule could be located in the pores from powder diffraction data. This discrepancy could be explained by a high dependence of the water content of CAU-1 on environmental conditions. The second weight loss is due to the decomposition of the aminoterephthalic acid from the framework and starts at approximately 310°C (Figure S4 in the Supporting Information). These results are in good agreement with the elemental analysis and with the temperature-dependent XRD measurements, which do not indicate any change in crystallinity or phase transitions up to 360°C. Above this temperature the framework collapsed. In comparison to flexible MOFs such as MIL-53, CAU-1 shows no structural changes upon dehydration. This thermal stability and the rigidity of CAU-1 could be

due to the presence of exclusively triangular windows in combination with the presence of the trivalent metal ions.

The permanent porosity has been confirmed by gas sorption measurements. The sorption isotherm (Figure 5) of CAU-1 exhibits type 1 behavior. The Langmuir surface area is approximately $1700 \text{ m}^2 \text{ g}^{-1}$, and a micropore volume of $0.52 \text{ cm}^3 \text{ g}^{-1}$ was determined.

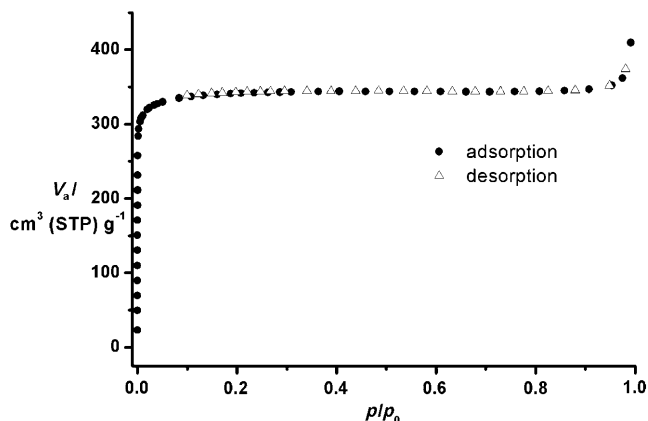


Figure 5. N_2 sorption isotherm of CAU-1 activated overnight at 130°C before measurement.

In conclusion, the field of formation of the new Al-based MOF $[\text{Al}_4(\text{OH})_2(\text{OCH}_3)_4(\text{H}_2\text{N-bdc})_3] \cdot x \text{H}_2\text{O}$ (CAU-1) has been determined using high-throughput methods. The structure contains unprecedented octameric $\{\text{Al}_8(\text{OH})_4(\text{OCH}_3)_8\}^{12+}$ building units, which are connected through the aminoterephthalate ions to a 12-connected net. CAU-1 exhibits high porosity and thermal stability. These properties in combination with the presence of the amino groups allow postsynthetic modification reactions. These results will be presented in a separate publication.

Experimental Section

The discovery and optimization of the synthesis of CAU-1 was investigated using our 24 multiclave (for details, see the Supporting Information). The optimized synthesis of CAU-1 in the 24-reactor system is as follows: a mixture of $\text{AlCl}_3 \cdot 6\text{H}_2\text{O}$ (92.7 mg, 0.384 mmol) and $\text{H}_2\text{N-H}_2\text{bdc}$ (23.32 mg, 0.129 mmol) was suspended in methanol (1.235 mL) and heated at 125°C for 5 h. Scale-up of the reaction to the gram scale was performed in a 250 mL Duran screw-cap glass bottle (Schott). $\text{H}_2\text{N-H}_2\text{bdc}$ (2.33 g, 12.9 mmol) and $\text{AlCl}_3 \cdot 6\text{H}_2\text{O}$ (9.27 g, 38.4 mmol) were suspended in methanol (123 mL). The resulting dispersion was heated at 125°C for 5 h.

After filtration, a yellow microcrystalline product was obtained. The as-synthesized product contains large amounts of chloride ions, which can be removed by stirring the microcrystalline product three times in deionized water (2000 mL per 0.5 g CAU-1) overnight. The product was isolated and dried at room temperature in air. Elemental analysis of the dehydrated phase $[\text{Al}_4(\text{OH})_2(\text{OCH}_3)_4(\text{H}_2\text{N-bdc})_3]$ ($M = 803 \text{ g mol}^{-1}$) calcd (%): C 42.35, H 3.83, N 5.32; found (%): C 41.85, H 3.64, N 5.23. Thermogravimetric analysis of the hydrated phase $[\text{Al}_4(\text{OH})_2(\text{OCH}_3)_4(\text{H}_2\text{N-bdc})_3] \cdot 3\text{H}_2\text{O}$: calcd weight loss 6.3%; found: 6.2%.

High-throughput X-ray analysis was carried out using a STOE high-throughput powder diffractometer. High-resolution X-ray

powder diffraction data used for the structural determination were collected on ID31 of the ESRF from a powdered sample.

^{15}N , ^{13}C , and ^1H solid-state NMR spectroscopic studies were performed on a commercial BRUKER DSX Avance 400 spectrometer operating at 9.4 T with resonance frequencies of 40.5, 100.7, and 400.1 MHz. ^1H and ^{13}C shifts were referenced relative to TMS and ^{15}N shifts to nitromethane. The samples were filled in 4 mm ZrO_2 rotors, mounted in a double-resonance probe (Bruker), and rotated with spinning frequencies of 8–12 kHz. A ramped cross-polarization sequence with contact times between 5 and 20 ms was employed to excite both the ^{13}C and ^{15}N nuclei via the proton bath. All 1D experiments were recorded using broadband proton decoupling by the SPINAL64 sequence.

Carbon, hydrogen, and nitrogen contents were determined by elemental chemical analysis on a Eurovektor EuroEA Elemental Analyzer. For more details, see the Supporting Information.

Received: March 13, 2009

Published online: June 5, 2009

Keywords: organic–inorganic hybrid composites · high-throughput methods · metal–organic frameworks · microporous materials · solvothermal synthesis

- [1] G. Férey, *Chem. Soc. Rev.* **2008**, 37, 191.
- [2] S. Kitagawa, R. Kitaura, S. Noro, *Angew. Chem.* **2004**, 116, 2388; *Angew. Chem. Int. Ed.* **2004**, 43, 2334.
- [3] J. L. C. Rowsell, O. M. Yaghi, *Microporous Mesoporous Mater.* **2004**, 73, 3.
- [4] G. Férey, C. Mellot-Draznieks, C. Serre, F. Millange, J. Dutour, S. Surblé, I. Margiolaki, *Science* **2005**, 309, 2040.
- [5] S. S.-Y. Chui, S. M.-F. Los, J. P. H. Charmant, A. G. Open, I. D. Williams, *Science* **1999**, 283, 1148.
- [6] M. Eddaoudi, J. Kim, N. Rosi, D. Vodak, J. Wachter, M. O’Keeffe, O. M. Yaghi, *Science* **2002**, 295, 469.
- [7] H. Li, M. Eddaoudi, M. O’Keeffe, O. M. Yaghi, *Nature* **1999**, 402, 276.
- [8] S. Surblé, C. Serre, C. Mellot-Draznieks, F. Millange, G. Férey, *Chem. Commun.* **2006**, 284.
- [9] C. Serre, C. Mellot-Draznieks, S. Surblé, N. Audebrand, Y. Filinchuk, G. Férey, *Science* **2007**, 315, 1828.
- [10] S.-T. Zheng, J. Zhang, G.-Y. Yang, *Angew. Chem.* **2008**, 120, 3903; *Angew. Chem. Int. Ed.* **2008**, 47, 3843.
- [11] S. Bauer, C. Serre, T. Devic, P. Horcajada, J. Marrot, G. Férey, N. Stock, *Inorg. Chem.* **2008**, 47, 7568.
- [12] A. Sonnauer, F. Hoffmann, M. Fröba, L. Kienle, V. Duppele, M. Thommes, C. Serre, G. Férey, N. Stock, *Angew. Chem.* **2009**, 121, 3849; *Angew. Chem. Int. Ed.* **2009**, 48, 3791.
- [13] S. Bauer, N. Stock, *Angew. Chem.* **2007**, 119, 6981; *Angew. Chem. Int. Ed.* **2007**, 46, 6857.
- [14] A. Sonnauer, N. Stock, *Eur. J. Inorg. Chem.* **2008**, 5038.
- [15] R. Banerjee, A. Phan, B. Wang, C. Knobler, H. Furukawa, M. O’Keeffe, O. M. Yaghi, *Science* **2008**, 319, 939.
- [16] M. P. Forster, N. Stock, K. A. Cheetham, *Angew. Chem.* **2005**, 117, 7780; *Angew. Chem. Int. Ed.* **2005**, 44, 7608.
- [17] N. Stock, T. Bein, *Angew. Chem.* **2004**, 116, 767; *Angew. Chem. Int. Ed.* **2004**, 43, 749.
- [18] T. Loiseau, C. Serre, C. Huguénard, G. Fink, F. Taulelle, M. Henry, T. Bataille, G. Férey, *Chem. Eur. J.* **2004**, 10, 1373.
- [19] T. Loiseau, L. Lecroq, S. Volkringer, J. Marrot, G. Férey, M. Haouas, F. Taulelle, S. Bourrelly, P. L. Llewellyn, M. Latroche, *J. Am. Chem. Soc.* **2006**, 128, 10223.
- [20] C. Volkringer, D. Popov, T. Loiseau, N. Guillou, G. Férey, M. Haouas, F. Taulelle, C. Mellot-Drazniek, M. Burghammer, C. Riekel, *Nat. Mater.* **2007**, 6, 760.
- [21] A. Comotti, S. Bracco, P. Sozzani, S. Horike, R. Matsuda, J. Chen, M. Takata, Y. Kubota, S. Kitagawa, *J. Am. Chem. Soc.* **2008**, 130, 13664.
- [22] T. Loiseau, C. Mellot-Draznieks, H. Muguerra, G. Férey, M. Haouas, F. Taulelle, *C. R. Chim.* **2005**, 8, 765.
- [23] I. Senkovska, F. Hoffmann, M. Fröba, J. Getzschmann, W. Böhlmann, S. Kaskel, *Microporous Mesoporous Mater.* **2009**, 122, 93.
- [24] T. Ahnfeldt, D. Gunzelmann, T. Loiseau, D. Hirsemann, J. Senker, G. Férey, N. Stock, *Inorg. Chem.* **2009**, 48, 3057.
- [25] J. Gascon, U. Aktay, M. D. Hernandez-Alonso, G. P. M. van Klink, F. Kapteijn, *J. Catal.* **2009**, 261, 75.
- [26] S. Couck, J. F. Denayer, G. V. Baron, T. Rémy, J. Gascon, F. Kapteijn, *J. Am. Chem. Soc.* **2009**, 131, 6326.
- [27] CCDC 723320 contains the supplementary crystallographic data for this paper. These data can be obtained free of charge from The Cambridge Crystallographic Data Centre via www.ccdc.cam.ac.uk/data_request/cif. Crystal data for $[\text{Al}_4(\mu\text{-OH})_2(\mu\text{-OCH}_3)_4(\text{H}_2\text{N-bdc})_3]\cdot\text{H}_2\text{O}$ (check 821.5 g mol^{-1}): tetragonal, $I4/mmm$, $a = b = 1835.17(1)$, $c = 1777.20(1)$ pm, $V = 5985.33(8) \times 10^6$ pm³, $Z = 4$. At the final stage, the Rietveld refinement involved the following parameters: 30 atomic coordinates, 5 thermal factors, 1 scale factor, 1 zero point, 2 cell parameters, 20 background parameters, and 8 parameters to model the evolution of diffraction lines shape. Soft restraints were maintained on the C–N and a few C–C bond lengths and C–C–N angles. The final Rietveld plot (Figure 3) corresponds to satisfactory crystal structure model indicator ($R_{\text{Bragg}} = 0.025$) and profile factors ($R_p = 0.053$ and $R_{\text{wp}} = 0.070$).
- [28] Topas V4.1: General Profile and Structure Analysis Software for Powder Diffraction Data Bruker AXS Ltd, **2004**.
- [29] A. Altomare, M. C. Burla, M. Camalli, B. Carrozzini, G. L. Casciarano, C. Giacovazzo, A. Guagliardi, A. G. G. Moliterni, G. Polidori, R. Rizzi, *J. Appl. Crystallogr.* **1999**, 32, 339.
- [30] A. Altomare, M. C. Burla, G. Casciarano, C. Giacovazzo, A. Guagliardi, A. G. G. Moliterni, G. Polidori, *J. Appl. Crystallogr.* **1995**, 28, 842.
- [31] A. Altomare, M. C. Burla, M. Camalli, G. L. Casciarano, C. Giacovazzo, A. Guagliardi, A. G. G. Moliterni, G. Polidori, R. Spagna, *J. Appl. Crystallogr.* **1999**, 32, 115.
- [32] A more detailed description of the crystal structure is given in the Supporting Information.
- [33] H. Kumagai and S. Kitagawa, *Chem. Lett.* **1996**, 471.
- [34] R. H. Laye, M. Murrie, S. Ochsenein, A. R. Bell, S. J. Teat, J. Raftery, H.-U. Güdel, E. J. L. McInnes, *Chem. Eur. J.* **2003**, 9, 6215.
- [35] M. Eshel, A. Bino, I. Felner, D. C. Johnston, M. Luban, L. L. Miller, *Inorg. Chem.* **2000**, 39, 1376.
- [36] C. Canada-Vilalta, M. Pinkand G. Christou, *Chem. Commun.* **2003**, 1240.
- [37] X.-M. Zhang, R.-Q. Fang, H.-S. Wu, *J. Am. Chem. Soc.* **2005**, 127, 7670.
- [38] D. Li, R. Wu, X.-P. Zhou, R. Zhou, X.-C. Huang, *Angew. Chem.* **2005**, 117, 4247; *Angew. Chem. Int. Ed.* **2005**, 44, 4175.
- [39] J. Jia, X. Lin, C. Wilson, A. J. Blake, N. R. Champness, P. Hubberstey, G. Walker, E. J. Cussen, M. Schröder, *Chem. Commun.* **2007**, 840.
- [40] J. H. Cavka, S. Jakobsen, U. Olsbye, N. Guillou, C. Lamberti, S. Bordiga, K. P. Lillerud, *J. Am. Chem. Soc.* **2008**, 130, 13850.